Applied Energy 211 (2018) 1343–1358

Contents lists available at ScienceDirect

Applied Energy

journal homepage: www.elsevier.com/locate/apenergy

Using machine learning techniques for occupancy-prediction-based cooling control in office buildings

Yuzhen Peng[a,*], Adam Rysanek[a], Zoltán Nagy[b], Arno Schlüter[a]

[a] Architecture and Building Systems, Institute of Technology in Architecture, Department of Architecture, ETH Zürich, Switzerland
[b] Intelligent Environments Laboratory, Department of Civil, Architectural, and Environmental Engineering, The University of Texas at Austin, USA

HIGHLIGHTS

- A new framework with multi-learning processes and specified rules is introduced for demand-driven cooling controls.
- The proposed control can automatically adapt to occupancy scenarios without prior calibration and knowledge.
- 7–52% energy savings were achieved in case study offices as compared to scheduled cooling operations.

ARTICLE INFO

Keywords:
Machine learning
Occupant behavior
Building control
Smart buildings
Energy savings

ABSTRACT

Heating, ventilation, and air-conditioning (HVAC) are among the major energy demand in the buildings sector globally. Improving the energy efficiency of such systems is a critical objective for mitigating greenhouse gas emissions and transitioning towards renewable sources of energy supply. The interest of this paper is to explore means to increase the efficiency of HVAC systems in accommodating occupants' behavior in real time. For instance, rooms in office buildings are not always occupied by occupants during scheduled HVAC service periods. This offers an opportunity to reduce unnecessary energy demands of HVAC systems associated with occupants' behavior. An in-depth analysis of occupants' stochastic behavior within an office building is conducted in this paper. A demand-driven control strategy is proposed that automatically responds to occupants' energy-related behavior for reducing energy consumption and maintains room temperature for occupants with similar performances as a static cooling. In this control strategy, two types of machine learning methods – unsupervised and supervised learning – are applied to learn occupants' behavior in two learning processes. The occupancy-related information learned by the algorithms is used by a set of specified rules to infer real-time room setpoints for controlling the office's space cooling system. This learning-based approach intends to reduce the need for human intervention in the cooling system's control. The proposed strategy was applied to control the cooling system of the office building under real-world conditions. Eleven case study office spaces were selected, representing three typical office uses: single person offices, multi-person offices, and meeting rooms. The experimental results report between 7% and 52% energy savings as compared to the conventionally-scheduled cooling systems.

1. Introduction

Globally, buildings account for approximately one-third of total final energy consumption [1]. Certain uses – heating, ventilation, and air-conditioning (HVAC) – are major consumers of energy and account for about 40% of total energy consumption in buildings [2]. Especially in extreme climates, such as the tropical weather of Singapore, air-conditioning systems are operated throughout the year, accounted for over 50% of the building stock's electricity consumption in these regions [3].

Occupants' behavior within buildings is a significant element affecting energy consumption [4]. For office buildings, rooms are not always fully occupied by occupants during daytimes, and some rooms are routinely unoccupied. For example, Mahdavi et al. [5] collected occupancy data from 48 offices of 3 university buildings in Austria, consisting of 41 single person offices and 7 multi-person offices (i.e. 6 rooms with 2 occupants and 1 room with 3 occupants). Results indicated that average occupancy rates of these offices were rarely over 60% according to calculated 24-h occupancy probability profiles. In another office building located in Singapore, Peng et al. [6] used

* Corresponding author.
E-mail address: yuzhen.peng@arch.ethz.ch (Y. Peng).

https://doi.org/10.1016/j.apenergy.2017.12.002
Received 30 July 2017; Received in revised form 25 November 2017; Accepted 1 December 2017

Nomenclature

Abbreviations

HVAC	heating, ventilation, and air-conditioning
ANN	artificial neural network
SVM	support vector machine
CO_2	carbon dioxide
HMM	Hidden Markov Model
KNN	K-nearest neighbor
PID	proportional, integral, and derivative
RBC	rule-based control
BMS	building management station
HMI	human-machine interface
PCB	passive chilled beam

Symbols (unit)

Y_{glbl}	global training dataset
n_{glbl}	size of the global training dataset
z_x	the number of unoccupied days in the past x days
$Z_{n_{td}}$	the number of days that an office is vacant in the training dataset
$Y_{lcl,j}$	a local training dataset
$a_{j,min}$	minimum value of daily first arrival in a local training dataset
$a_{j,max}$	maximum value of daily first arrivals in a local training dataset
$dev_{j,arr}$	deviation of daily first arrival in a local training dataset
n_j	size of the evaluated training set
$v_{j,max}$	value of daily maximum vacancy duration during working hours
$v_{j,thrd}$	a threshold value of maximum vacancy durations
$CM(occ, v_{shrt})$	control mode
k_{pttrn}	the number of occupancy patterns
a_{cur}	a valid time of the first arrival
$v_{cur,max}$	maximum vacancy duration of working hours in the current day
Y_{td}	final training dataset
$t_{prdct,np}$	time of occupants' next presence
$t_{prdct,drtn}$	total presence duration for the rest of the day
$NN(k_{KNN}, y_{cur}, Y_{td})$	k_{KNN} nearest neighbors
y_{cur}	current-day occupancy vector
$y_{cur,n}$	value in the n-th bit of y_{cur}
n_{td}	size of the training dataset
$y_{td,m}$	a sample in the training dataset
$y_{td,mn}$	value in the n-th bit of $y_{td,m}$
p_{thrd}	a threshold value
$T_{sp,cmf}$	comfort temperature setpoint
$T_{sp,dl}$	idle temperature setpoint
$T_{sp,ddl}$	deep idle temperature setpoint
	economy temperature setpoint
$t_{dcc,strt}$	time at which the DCC starts to infer temperature setpoints
$t_{dcc,stp}$	time at which the facility department switches off cooling services
$t_{arr,thrd}$	threshold value of cumulative probability of daily first arrivals
$t_{dprtr,thrd}$	threshold value of cumulative probability of daily last departures
$t_{drtn,thrd1}$ and $t_{drtn,thrd2}$	threshold value of presence durations
$t_{sg,j}$	time segment
$E_{chgMd,drtn<3}$	cooling energy consumed by modifying temperature setpoints from $T_{sp,dl}$ and $T_{sp,ddl}$ to the comfort mode for short stays
t_{dprtr}	daily last departure

motion sensors to detect occupants' behavior in 6 offices over a seven-month period. These offices included 4 single person offices and 2 multi-person offices (i.e. one room with 2 occupants and one room with 4 occupants). They found that the single person offices had low occupancy rates – daily peak occupancy probability only touched about 60%, and the multi-person offices had higher occupancy likelihoods – their peak occupancy rates were about 90%. However, equipment in buildings normally keeps in operation without considering actual occupancy of offices. This causes unnecessary energy usage during non-occupied periods. Masoso et al. [7] reported that energy consumed in non-occupied hours is more than that used in occupied hours – 56% and 44%, respectively. They mentioned that this was primarily caused by keeping office equipment in operation until the end of each day, irrespective of occupancy patterns. Nguyen et al. [8] also indicated occupants' energy-unconscious behavior resulted in about one-third more energy consumption in buildings.

In the building sector, upgrading the energy efficiency of HVAC systems is a critical objective for developing a low-carbon economy. An approach to reduce energy-related carbon emission in principle is to decrease energy demand [9,10]. From a control science point of view, a better understanding of occupants' behavior is a critical component to achieve this goal. To reduce unnecessary energy requirements and maintain comfortable indoor temperatures for occupants, one group of control strategies make air-conditioning systems adapt to occupants' actual energy-related behavior instead of static operation schedules specified by the facility departments of the buildings. These demand-driven control strategies switch HVAC systems to setback modes with adjusting indoor climate setpoints (i.e. room temperature, humidity, and carbon dioxide concentration) during unoccupied hours. When office spaces they serve are being occupied again, the demand-driven controls switch the systems back to comfort modes.

Central to developing a demand-driven HVAC control strategy is time-varying data on current and upcoming occupancy. Real-time occupancy can be measured or inferred from sensor networks installed in perceived rooms. Prominent real-time occupancy detection in commercial office buildings are reviewed by Labeodan et al. [11]. Nevertheless, predicting occupancy of individual rooms in coming hours is a challenging task due to the fact that occupants' behavior is highly stochastic.

In prior HVAC control research, a group of machine learning techniques were explored and embedded into systems to infer necessary knowledge of outdoor and indoor climate, room occupancy, and occupants' thermal preferences [12]. These yielded promising results in improving energy savings and indoor thermal comfort. In this study, we focus mainly on occupancy demand-driven control with machine learning techniques.

Prior occupancy learning studies with machine learning techniques have represented and predicted occupants' behavior in different formats, such as binary data (i.e. presence and absence) [13–18], discrete values (i.e. the number of occupants) [19–28], or continuous data (i.e. probability distributions of occupancy) [29–31]. Two groups of machine learning algorithms – that is, supervised and unsupervised learning [32,33] – were exploited in this area. The former is utilized to learn room occupancy based on occupancy datasets collected from buildings. The latter is used to find occupancy patterns.

To predict occupants' presence for a domestic heating control system, the ACHE project [13] developed an occupancy predictor to learn occupancy data transformed from motion signals. Researchers in this project tested three different occupancy predictor approaches: a lookup table, a backpropagation artificial neural network (ANN), and a

backpropagation ANN with a look-up table, respectively. Test results showed the ANN with look-up table generated the best prediction of the three. Another residential heating application developed by Scott et al. [14] used a k-nearest neighbor (KNN) algorithm to forecast occupants' presence based on datasets collected from radio frequency identification devices and motion sensors. Their test results showed that total gas usage for heating reduced by 8% to 18% by using the forecasted presence information to preheat entire houses. Some studies focus on modeling occupants' presence and absence in monitored spaces with machine learning algorithms. Kadouce et al. [15] used a support vector machine (SVM) classifier to infer occupants' presence and absence with learning sensory datasets from motion sensors, pressure detectors, lamps, door and switch contactors, and flow meters. Sangogboye et al. [16] modeled occupants' presence with machine learning techniques based on motion data from two commercial buildings, and SVM indicated robust performance according to their result. Ortega et al. [17] used SVM to model occupants' presence and activity patterns based on data collected from motion, pressure and contact sensors in 3 houses. ANN, KNN, and SVM were used as supervised learning in the above studies. Chaney et al. [18] evaluated occupants' presence and vacancy status with Hidden Markov Model (HMM) based on data of electrical power, carbon dioxide (CO_2) levels, and room dew point.

For controlling a heating and cooling system in an academic house, Dong's HVAC control testbed [19,20] embedded a function to predict the number of occupants. It used a Gaussian Mixture Model to classify changes of selected features derived from data on sound, light, motion, CO2 concentration, temperature, and relative humidity. It then employed a supervised learning algorithm (i.e. HMM) to estimate the number of occupants. The experimental result showed 26% and 17.8% heating and cooling energy saved, respectively, when compared to a scheduled control operation. In another study, Wang et al. [21] also integrated profiles of the number of occupants to effectively control an HVAC system. They used a feature-scaled ANN to generate profiles of the number of occupants in an office of City University of Hong Kong based on image datasets collected from cameras. Their simulation result indicated 20% energy saved. Some studies modeled the number of occupants in buildings with machine learning algorithms. Ryu et al. [22] proposed a predictor of the number of occupants with HMM, using data of CO_2 concentration, energy use of lighting systems and appliances collected from a test-bed. Yang et al. [23] utilized an ANN with a radial basis function as the supervised learning to estimate the number of occupants in an educational building from mining data of indoor temperature, humidity, CO_2 level, illumination, acoustics, and occupants' movements. Mamidi et al. [24] exploited machine learning techniques to predict the number of occupants for an open office. Their results indicated that ANN achieved better performance based on learning data of motion, CO_2 concentration, sound level, light, and door state. For another open space, Ekwevugbe et al. [25] also used ANN to infer the number of occupants based on sound data, indoor temperature, and motion detection. Chen et al. [26] modeled occupancy level based on data collected from a building in the University of Florida campus, ANN and SVM showed superior performance for predicting the number of occupants during the forecast time frame of 2 h. Liang et al. [27] proposed an approach that firstly clustered occupancy patterns with an unsupervised learning algorithm (i.e. k-means), and then it learned rules with a supervised learning algorithm (i.e. decision tree) to infer daily profiles of the number of occupants in a building. Recently, Capozzoli et al. [28] employed the similar process with k-means and decision tree to mode occupancy profile (i.e. the number of occupants) for reducing energy consumption of HVAC systems. Their simulation result suggested a 14% energy saving potential in comparison to a static operation schedule.

To control indoor household temperatures in a simulation-based platform, Lu et al. [29] utilized an HMM to predict probabilities of occupant departures, arrivals, and sleeping by learning from datasets collected from motion and door sensors. Their results showed average cooling and heating energy savings of 28%. For another household heating control study based on a simulated platform, Kleiminger et al. [30] employed machine-learning-based approaches proposed in [14,29] (i.e. KNN and HMM) and a presence-probabilities-based strategy presented in [34] to predict occupants' arrivals. Their occupancy data was derived from 45 individuals' mobile phone records, and simulated results indicated annual energy savings of 6% to 17%. To model occupancy schedules of an academic building based on the format of daily probability distributions, D'Oca et al. [31] proposed a three-step framework using both supervised learning and unsupervised learning. In the first step, a supervised learning algorithm, decision tree, was employed to predict presence by learning occupancy datasets of a building. In the second step, a range of rules was generated by a rule induction algorithm according to the information from the previous step. Lastly, an unsupervised learning algorithm, k-means, was applied to cluster the similar patterns of occupancy schedules for that building.

The above studies, and their related works, provide valuable insights on exploring occupants' behavior in buildings using machine learning techniques. This study further explores occupancy demand-driven cooling controls using machine learning techniques, and exploits energy saving potentials in typical office scenarios. Scientific contributions of this study contain:

- A new framework with multi-learning processes and rule-based control is introduced for demand-driven cooling controls.
- The proposed methodology can make cooling systems automatically adapt to occupants' actual energy demand in different office contexts for saving energy without compromising room temperatures during occupied periods.
- To obtain realistic results and to validate the effectiveness of the control strategy in real-world applications, the proposed methodology is conducted in 11 existing office settings. These comprise three different and typical office types: single person offices, multi-person offices, and meeting rooms. The results are presented and discussed for each office type from five aspects.

The proposed methodology and the experimental results provide view and information on energy conservation of building systems. In the meantime, this study also demonstrates and discusses how this control strategy is deployed with a building management station (BMS) for real applications.

The subsequent sections of this paper are organized as follows. Section 2 presents the proposed methodology of demand-driven control in detail. Section 3 gives an introduction to the case study, including the case study space and experimental setup, analysis of occupancy-related data, and examples of control operation. Test results are illustrated upon implementing the proposed control strategy in Section 4. Lastly, Section 5 discusses and concludes the paper' findings.

2. Methodology

This study focuses on the demand-driven cooling control (DCC) with learning capabilities, following up our prior study [6]. For the approach introduced in this paper, more occupancy-related features are analyzed and integrated into the DCC. Furthermore, two algorithms are used to learn occupancy patterns and predict occupants' presence and presence duration for the remainder of a day based on room motion signals. The above strategies are integrated into this framework to enhance the control reliability against the occupants' stochastic behavior. Then the forecasted occupancy information is indirectly deployed to infer set-back setpoint temperatures according to a set of rules specified from our study. The holistic control strategy is illustrated in this section.

2.1. The block diagram of the whole control strategy

An overview of the proposed control strategy is given in Fig. 1. This

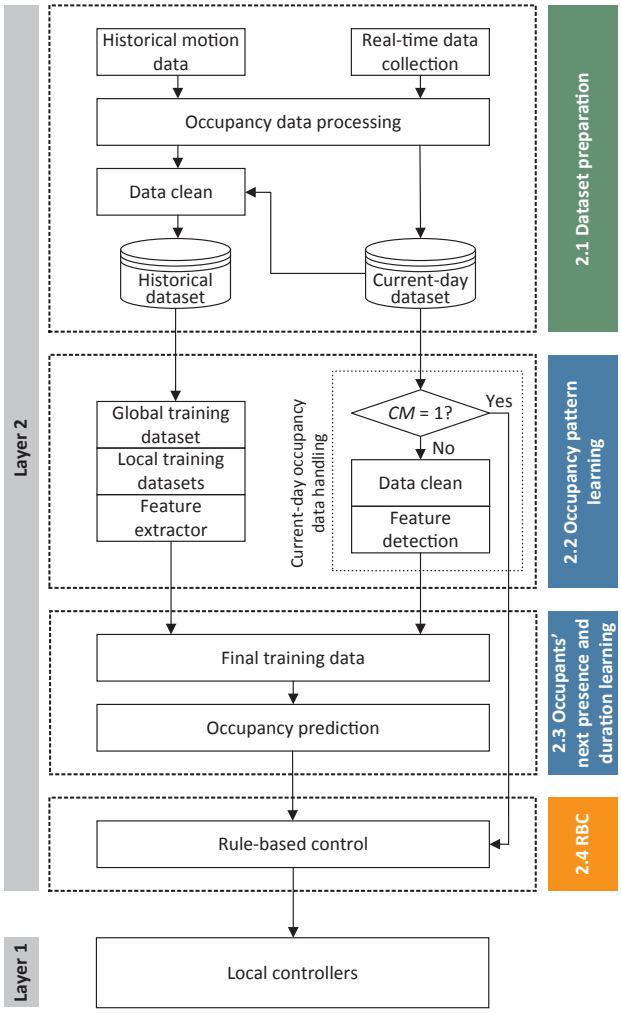

Fig. 1. Block diagram of the proposed control strategy.

consists of two layers. Local controllers with proportional, integral, and derivative (PID) algorithm in the first layer are mainly in charge of controlling cooling systems to ensure indoor temperatures at setpoint levels. The DCC is embedded in the second layer to specify temperature setpoints for the local controllers dynamically. The second layer makes the entire cooling system capable of adapting to actual energy demands relevant to occupants' behavior.

The remainder of this section mainly introduces the second layer in detail. It consists of four modules, including two learning processes with machine learning techniques:

- Module 2.1: Dataset preparation.
- Module 2.2: Occupancy pattern learning (first learning process).
- Module 2.3: Occupants' next presence and duration learning (second learning process).
- Module 2.4: Rule-based control (RBC).

2.2. Module 2.1: dataset preparation

The goal of this module is to create and clean occupancy datasets for two learning processes in the second layer.

In this study, we use motion sensors as devices to detect occupants' movements. Such sensors are normally provided in buildings featuring motion-controlling lighting systems, though the data from these sensors could be used for other building automation purposes. The data preparation module collects historical motion signals from motion sensors equipped in each target office before conducting the DCC into air-conditioning systems, and closely monitors real-time occupants' motions during the current day.

A time delay (TD) is required to interpret the motion data in terms of occupancy. The TD is a minimum time needed between two consecutive movements (i.e. inactive time slices) to assume that there are no occupants in the monitored spaces [35]. That is, if there is no movement within time-frames that are greater than or equal to TD, the space is assumed to be unoccupied. In this study, inactive time slices are extracted from 7.5-month motion datasets of case study rooms to specify the TD. Inactive durations of less than 100 ss and 10 mins account for over 97% and 98% of total inactive slices, respectively. In order to get a high confidence level of confirming occupants' vacancy, 10 mins is assigned to TD, which is consistent with prior studies [36,37]. In other words, the probability of vacancy is 2% of the total inactive slices. After converting motion singles to occupancy information, each occupancy vector contains a set of Boolean attribute data to represent occupancy status per minute: 1 means that a monitored room is occupied and 0 means that the room is not occupied. The formatted occupancy data is stored in two databases: a historical weekday dataset and a current-day dataset. At the end time of a weekday, the current-day occupancy vector is updated automatically to the historical dataset for the control on the next day.

In the meantime, invalid occupancy data in occupancy vectors is cleaned before saving the occupancy vector into the historical dataset. The invalid occupancy data includes short stays (i.e. presence duration is less than 3 mins) and a short daily first arrival (i.e. the first arrival shows up before a_{thrd} time point with less than d_{thrd} duration). a_{thrd} and d_{thrd} are assigned by analyzing distributions of historical first arrivals and durations of them. A data clean function is coded to compute all presence durations, and then filter time slices of short stays (i.e. set corresponding binary bits to 0). After cleaning short stays, the clean function calculates the time and duration of the first arrival in the occupancy vector, and sets corresponding bits to 0 when the daily first arrival meets the above criteria of the daily short first arrival.

Among them, a daily invalid first arrival with a short duration (i.e. d_{thrd}) is not valid for the DCC. That is because according to our observation and data analysis, the first short arrival before a_{thrd} in an office is normally triggered by staff who clean the space, or one occupant staying in the room briefly and then going to the pantry before returning to the space or going somewhere else for a meeting.

2.3. Module 2.2: occupancy pattern learning

In this module, we define two types of training datasets: a global training dataset and several local training datasets. The global training dataset is selected from the historical weekday dataset. The local training datasets are clustered from the global training set according to the specified number of occupancy patterns in individual rooms, and each training dataset represents a type of occupancy patterns in the global dataset.

The aim of this module is not only to prepare global and local training datasets, but also extract occupancy-related features from the local training datasets and an occupancy vector of the current day. Importantly, the datasets and parameters specified in this module are automatically updated once a day or every several minutes, mainly to make the DCC response to changes of occupants' stochastic behavior.

2.3.1. Global training dataset

The global training data (Y_{glbl}) is a set of daily occupancy vectors for previous weekdays. A major parameter of it is the size of the global training dataset (n_{glbl}). In order to make the DCC operation quickly respond to occupants' behavior changes as circumstances vary (e.g. full-load office work, business trips, holiday seasons, and new staff) as well as ensuring n_{glbl} is not small, we specify its value according to rules summarized in Table 1. The basic idea of this is to limit the number of valid days (i.e. a room is occupied in a day) in the global training data

Table 1
The mechanism for selecting the size of the global training dataset.

The number of days that an individual room is not occupied			The size of the global training dataset n_{glbl}
z_{20}	z_{30}	z_{40}	
$z_{20} < 4$			20
$5 \leqslant z_{20} \leqslant 10$	$z_{30} \leqslant 15$		30
$5 \leqslant z_{20} \leqslant 10$	$z_{30} > 15$		40
$z_{20} > 10$		$z_{40} \leqslant 20$	40
$z_{20} > 10$		$z_{40} > 20$	45

between 15 and 29. As shown in Table 1, the value of n_{glbl} is driven by the number of unoccupied days in the past 20, 30, and 40 weekdays (i.e. z_{20}, z_{30}, and z_{40}). However, in case a particular room is not occupied frequently, i.e., the number of unoccupied days is over 20 in the past 40 weekdays, the value of n_{glbl} is fixed to 45.

During the DCC operation, this vacancy-driven global training dataset is updated autonomously once a day in the early stage of the DCC operation.

2.3.2. Local training datasets

The first learning process in this study is embedded in this submodule, mainly to learning occupancy patterns from the global training data for clustering local training datasets.

In this study, we define four major categories of occupancy patterns, as shown in Fig. 2. The gray blocks in Fig. 2(a) indicate that occupants are present in rooms during those periods. Start and end times of the gray blocks in the timeline only indicate differences of the four occupancy patterns. Positions of them are not absolute values, differing in rooms as circumstances change. For the first occupancy pattern (i.e. pattern 1), rooms are occupied both in the morning and afternoon. Pattern 2 shows that occupants leave their offices early. Conversely, pattern 3 indicates that occupants tend to show up in their offices late. 'Early' and 'late' are relative to occupants' normal behavior. Lastly, 'no presence' in a day is defined as pattern 4. Four examples of the occupancy patterns in an office are shown in Fig. 2(b). The above analysis aims to limit the number of occupancy patterns (k_{pttrn}) for clustering local training datasets from the global dataset. In this study, k_{pttrn} therefore is limited to 4 when the global training dataset contains days with no occupants present (i.e. pattern 4), otherwise k_{pttrn} is set to 3.

According to vector-based occupancy profiles, we extract seven occupancy-related features as follows:

1. Day of the week.
2. Time of the daily first arrival.
3. Time of the daily last departure.
4. Daily total occupied duration.
5. The number of daily presence.
6. Daily maximum occupancy duration.
7. Daily maximum vacancy duration during working hours.

To reduce feature dimensionality for searching occupancy patterns, we employed a sequential feature selection [38] to extract the three most important occupancy-related features that shape daily occupancy profiles. Among the above seven features, three features – time of the daily first arrival, time of daily last departure, and daily maximum vacancy duration during working hours – are chosen by the sequential feature selection.

These three features are applied to two learning processes (i.e. module 2.2 and module 2.3). In this module, the global training dataset is divided into several training datasets according to clustered occupancy patterns. The daily occupancy range is shaped by the two most important features (i.e. the time of the daily first arrival and the time of the daily last departure). Meanwhile, learning and control purposes presented in Sections 2.4 and 2.5 are mainly related to occupants' behavior within the daily first arrival and last departure. Thus, two-dimensional data (X) consisting of these two features are retrieved from the global dataset for clustering the local training datasets. The time of the daily first arrival and the maximum daily vacancy duration during working hours are used in module 2.3 for selecting the final training data from the global and local training datasets according to the occupancy pattern of the current day.

To recognize the local training datasets from the above two-dimensional occupancy-related dataset with less human intervention, we employ an unsupervised learning algorithm that is k-means for clustering, rather than a supervised learning algorithm used for classification. The k-means clustering is a widely used unsupervised learning approach, seeking k clusters from a given dataset [39–41]. To cluster the local training datasets from the global training dataset, we deploy k-means with an optimization criterion in this module, as shown in Eq. (1).

$$p_i = \text{argmin}_j \|x_i - c_j\|^2 \tag{1}$$

The two-dimensional dataset (X) is shown in Eq. (2), and means of clusters (C) are presented in Eq. (3). x_i and c_j are samples of X and C, respectively. Allocating x_i to the closest cluster is computed by Eq. (1), and $\|\cdot\|^2$ represents the Euclidean square norm.

$$X = \{x_1,\ldots,x_m\}, \quad m = n_{glbl} \tag{2}$$

$$C = \{c_1,\ldots,c_k\}, \quad k = k_{pttrn} \tag{3}$$

The initial values of C are assigned randomly from the range of X. They are updated according to Eq. (4) in each iteration of allocating X to the closest clusters C, until the algorithm converges (i.e. assignments of clusters do not change too much).

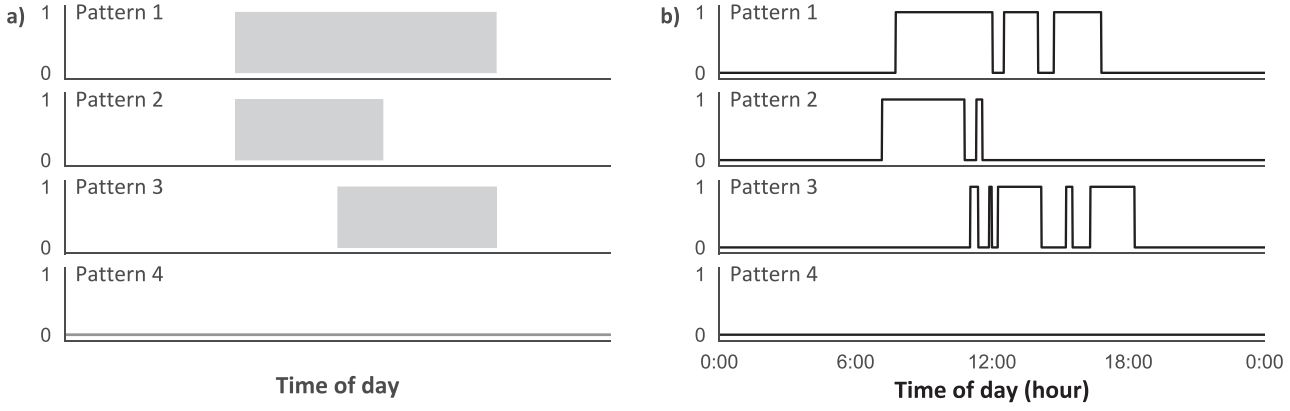

Fig. 2. Four types of occupancy patterns. (a) Formats of specified occupancy patterns, (b) examples of the occupancy patterns in an office.

Table 2
The mechanisms for selecting training data from the global and local training datasets.

Two occupancy-related features in the current day		The final training data (Y_{td})
The valid first arrival a_{cur}	The maximum vacancy duration of past working hours $v_{cur,max}$	
$a_{cur} = 0$		Y_{glbl}
$a_{cur} \notin [a_{j,r1}, a_{j,r2}]$		Y_{glbl}
$a_{cur} \in [a_{j,r1}, a_{j,r2}]$	$v_{cur,max} \leqslant v_{j,thrd}$	$Y_{lcl,j}$
$a_{cur} \in [a_{j,r1}, a_{j,r2}]$	$v_{cur,\max} > \max(v_{j,thrd})$	Y_{glbl}

$$c_j = \frac{\sum_i r_{ij} x_i}{\sum_i r_{ij}}, \quad r_{ij} = \begin{Bmatrix} 1, & p_i = j \\ 0, & p_i \neq j \end{Bmatrix} \tag{4}$$

Occupancy clusters recognized from the above process portions the global training dataset into k_{pttrn} sets of local training datasets ($Y_{lcl,j}$), as presented in Eq. (5):

$$Y_{lcl,j} = \bigcup_1^{n_{glbl}} x_i,\ p_i = j \tag{5}$$

2.3.3. Feature extractor

The objectives of the proposed methodology not only make it is possible for the DCC to learn from occupants' original presence and vacancy, but also incorporate deviations of occupancy-related features to improve the reliability of control against occupants' stochastic behavior. Therefore, the feature extraction in this submodule mainly focuses on retrieving occupancy-related features from each particular local training dataset $Y_{lcl,j}$ and using them to get two parameters associated with behavior deviations.

The first two features of a local training dataset are the minimum and maximum values of daily first arrivals, represented by $a_{j,min}$ and $a_{j,max}$, respectively. The third feature is a deviation value of the daily first arrivals ($dev_{j,arr}$), as shown in Eq. (6). Where, n_j is the size of the evaluated local training dataset. The last feature is the value of daily maximum vacancy durations during working hours ($v_{j,max}$).

$$dev_{j,arr} = \begin{Bmatrix} \max\left\{\frac{a_{j,max} - a_{j,min}}{n_j}, 20\right\}, & n_j > 1 \\ 0, & n_j = 1 \end{Bmatrix} \tag{6}$$

According to the above local-training-dataset-based features, two key parameters are computed from them. The first one represents a time range between $a_{j,r1}$ and $a_{j,r2}$: $[a_{j,r1}, a_{j,r2}]$. $a_{j,r1}$ and $a_{j,r2}$ are calculated according to Eqs. (7) and (8), respectively.

$$a_{j,r1} = a_{j,min} - dev_{j,arr} \tag{7}$$

$$a_{j,r2} = a_{j,max} + dev_{j,arr} \tag{8}$$

The second one is a threshold value of the maximum vacancy durations ($v_{j,thrd}$), defined in Eq. (9).

$$v_{j,thrd} = v_{j,max} + 20 \tag{9}$$

2.3.4. Handling of the current-day occupancy information

This submodule mainly handles current-day occupancy data. If an office is occupied (i.e. $occ = 1$) or the room is only unoccupied ($occ = 0$) in a specified short period (i.e. $v_{shrt} = 1$), the control jumps directly to the RBC in the module 2.4 to call a comfort mode operation ($CM = 1$) for maintaining room temperatures at assumed comfortable levels with comfort setpoints. Otherwise, the DCC enters into a setback mode ($CM = 0$) and the data clean function presented in Module 2.1 is executed. The notation $CM(occ, v_{shrt})$ denotes the control modes (i.e. comfort and setback modes) during the control operation. As shown in Eq. (10), it is determined by the current occupancy status and an indicator of whether the current vacancy is short or not.

$$CM(occ, v_{shrt}) = \begin{Bmatrix} 1, & occ = 1 \\ 1, & occ = 0 \text{ and } v_{shrt} = 1 \\ 0, & \text{otherwise} \end{Bmatrix} \tag{10}$$

For occupancy in the current day, a feature-detection function is deployed to monitor and compute a valid time of the first arrival (a_{cur}) and the maximum vacancy duration of past working hours ($v_{cur,max}$).

In contrast to previous submodules in module 2.2 that are computed spontaneously per day, the current-day occupancy data in this submodule runs in each control cycle.

2.4. Module 2.3: occupants' next presence and duration learning

The module presented in this section chooses final training data from the global and local datasets, and uses a supervised machine learning algorithm to learn and predict occupants' next presence and presence duration for the remainder of a day based on the selected final training data and the detected occupancy information in the current day. This module is only executed by the DCC when zero is assigned to $CM(occ, v_{shrt})$.

2.4.1. Final training data selection

The global and local training datasets specified by Module 2.2 are not assigned as training data for the occupancy learning process of Module 2.3 directly. The final training data (Y_{td}) is used as the training data in this learning process, which is selected from the global or local training datasets according to mechanisms presented in Table 2. The time of the daily first arrival and the maximum daily vacancy duration during working hours are employed by Table 2 to make decisions of specifying the final training data, including a_{cur} and $v_{cur,max}$ of the current day, $[a_{j,r1}, a_{j,r2}]$ and $v_{cur,max}$ of the local datasets.

If a_{cur} keeps the initial state (i.e. zero) or does not falls into the range of $[a_{j,r1}, a_{j,r2}]$, the global training dataset is assigned as final training data. When a valid a_{cur} is perceived in the current day and falls into one or more $[a_{j,r1}, a_{j,r2}]$, $v_{cur,max}$ is used to judge whether to choose local training datasets or only to use the global training dataset as the final training data. If $v_{cur,max}$ is larger than threshold values $v_{j,thrd}$ of selected local training datasets, we regard the current occupancy pattern as deviating from patterns in these local training datasets, and the global training dataset is restored as the final training data. Otherwise, one or more local training datasets corresponding to matched $[a_{j,r1}, a_{j,r2}]$ are employed as Y_{td}. As the values of a_{cur} and $v_{cur,max}$ vary in line with occupants' behavior in the current day, Y_{td} is recalculated during the execution of module 2.3.

2.4.2. Occupancy prediction

The second learning process based on the machine learning techniques is embedded in this module. Inspired by [14] and further exploited in our prior research [6], a supervised machine learning algorithm – k-nearest neighbor (KNN) – is deployed in this study to predict occupancy information.

For the DCC, whether occupants will be present in an office or not indicates whether the cooling service is required or not. Meanwhile, diminishing presence duration in the remaining day also implies that an office tends to be unoccupied. The forecasted occupancy information, therefore in this study, consists of time of the occupants' next presence ($t_{prdct,np}$) and total presence duration in the remaining day ($t_{prdct,drtn}$).

The KNN is usually used to seek k pieces of data from training dataset that are most similar to a piece of new information, with computing distance between the new data and each sample in the training dataset. Then the k-most-similar samples are assigned to the new data for purposes of regression or classification [39,42].

In this study, the notation $\mathrm{NN}(k, y_{cur}, Y_{td})$ represents a group of k nearest neighbors that obtained from the final training data Y_{td} for the current-day occupancy vector (y_{cur}). For computing $\mathrm{NN}(k, y_{cur}, Y_{td})$, the value of k need to be assigned. Too large or too small value of k will

make the algorithm overestimate or underestimate occupants' next presence and presence duration for the rest of the day. This value is normally determined by fine tuning via trial-and-error or using cross-validation [14,43]. According to the pre-study based on the simulation, we summarize a set of rules together with two formulas to specify the value of k in this work, as shown in Table 3. $Z_{n_{td}}$ represents the number of days that an office is vacant in the final training data.

The final training data and the current-day occupancy data for each room are binary vectors. So the Hamming distance [44] that identifies the number of bits on which the two binaries differ is employed to determine the k-most-closest neighbors of the current-day occupancy data. The Hamming distance of them is defined as in Eq. (11).

$$d(y_{cur}, y_{td,m}) = \sum_{n=1}^{t} \{y_{cur,n} \neq y_{td,mn}\} \tag{11}$$

where y_{cur} is a t-bit vector, carrying the occupancy status of the current day from 00:00 to the sampling point (i.e. t in minute). $y_{cur,n}$ is the value in the n-th bit of y_{cur}. $y_{td,m}$ denotes a daily occupancy sample in the training dataset (Y_{td}), and $y_{td,mn}$ is the value in the n-th bit of $y_{td,m}$.

After getting NN(k, y_{cur}, Y_{td}) with the Hamming distance computation, fragments of the k-most-closest samples corresponding to remaining minutes in the current day are tailored to compute the occupancy probability of each remaining bit. Then, a threshold value (p_{thrd}) is required to transform the occupancy-probability-based vector to a binary-based occupancy vector. p_{thrd} is a constant value that can be defined between zero to one, and we set it to zero due to ensuring the comfortable indoor temperature for occupants is the highest priority in this study. This way, presence in a bit of the occupancy vector is stated once the occupancy probability in that bit is greater than zero. p_{thrd} can also be assigned to a larger value to achieve a more energy-conscious purpose.

This partial occupancy vector is assigned to the rest of the current day as the predicted occupancy vector. In the last step of this sub-module, predicted occupancy information $t_{prdct,np}$ and $t_{prdct,drtn}$ are computed from it.

2.5. Module 2.4: Rule-Based Control (RBC)

Module 2.4 aims to infer time-dependent room temperature setpoints for local controllers. This section illustrates this module from two aspects: (1) definition of the comfort and setback modes, (2) rules of determining temperature setpoints of comfort and setback modes.

To start, two control modes with four temperature setpoints are defined for the DCC. When a room is occupied or is only vacant in a short period as explained in Section 2.3.4, the comfort temperature setpoint ($T_{sp,cmf}$) is sent to the local controllers to have cooling systems run at the comfort mode. Otherwise, the DCC process enters into the setback mode. Three temperature setpoints are deployed in the setback mode to achieve different levels of energy savings: idle temperature ($T_{sp,dl}$), deep idle temperature ($T_{sp,ddl}$), and economy temperature (). They are defined in Eqs. (12)–(14) as follows.

$$T_{sp,dl} = T_{sp,cmf} + 1\ [°C] \tag{12}$$

$$T_{sp,ddl} = T_{sp,dl} + 0.5\ [°C] \tag{13}$$

$$T_{sp,ecn} = 35\ [°C] \tag{14}$$

The main objectives of applying the above setback temperature setpoints are to reduce the cooling delivered to an office space step by step as the probability of occupants being present in the room goes down, and to maintain space temperature within the constraints until a point in time at which the confidence level is high enough that the room will not be occupied anymore on this day. We assume that an indoor temperature of $T_{sp,dl}$, 1 °C higher than the $T_{sp,cmf}$, is within an acceptable tolerance for occupants to represent the idle temperature. It is assigned to save cooling energy when a room is not occupied, but there is a modest probability that it will be occupied with a certain duration in the current day. is applied to shut down the cooling systems when occupants will not return to their rooms in the current day. The value of $T_{sp,ddl}$ is inserted between $T_{sp,dl}$ and . This setpoint releases a room's temperature to a higher level than $T_{sp,dl}$, as the likelihood of occupants being present in the room goes down. The purpose of this is to reduce cooling energy further compared to $T_{sp,dl}$, and at the same time, it limits room temperature not to rise too fast compared to .

To effectively use predicted $t_{prdct,np}$ and $t_{prdct,drtn}$ for the DCC operation, we also define another three sets of variables to formulate rules for the changeover room temperature setpoints of the setback mode:

1. Definitions of the DCC operation period
   One parameter is the time at which the DCC starts to infer the temperature setpoints ($t_{dcc,strt}$), the other is the time at which the facility department switches off the cooling systems ($t_{dcc,stp}$).
2. Statistical analysis of historical occupancy data
   Two threshold values are computed from cumulative probabilities of historical daily first arrivals and last departures: $t_{arr,thrd}$ and $t_{dprtr,thrd}$, respectively. In this study, $t_{arr,thrd}$ and $t_{dprtr,thrd}$ are set to the time points at which the cumulative probabilities of the first arrivals and the last departures are 95%.
   For a more energy-conscious perspective, these two values can be set to smaller values such as 90% or less. However, a value higher than 95% is not suggested since remaining 5% of first arrivals and last departures are considered abnormal behavior for the DCC [6].
3. Threshold values of presence durations: $t_{drtn,thrd1}$ and $t_{drtn,thrd2}$.

Four variables of the first two sets are time-based values in minutes, and two variables of the third set are quantitative parameters. The four time-based values divide a 24-h day into five ranges: $t_{sg,1}$ to $t_{sg,5}$, as shown in Eqs. (15)–(19). The daily first arrivals are mostly distributed in $t_{sg,1}$ and $t_{sg,2}$, and the daily last departures are mainly dispersed in $t_{sg,3}$ and $t_{sg,4}$.

$$t_{sg,1} = (1,\ t_{dcc,strt}] \tag{15}$$

$$t_{sg,2} = (t_{dcc,strt},\ t_{arr,thrd}) \tag{16}$$

$$t_{sg,3} = [t_{arr,thrd},\ t_{dcc,stp}] \tag{17}$$

$$t_{sg,4} = (t_{dcc,stp},\ t_{dprtr,thrd}] \tag{18}$$

$$t_{sg,5} = (t_{dprtr,thrd},\ 1440] \tag{19}$$

With the purpose of generalizing the DCC for requirements of diverse application scenarios, these three sets of variables are packaged into an initialization function that can be configured by end-users. In the last computation step of this module, the predicted $t_{prdct,np}$ and $t_{prdct,drtn}$ are used indirectly to infer setback temperature setpoints based on rules summarized in Table 4.

Table 3
The mechanism for calculating the value of k.

The final training data (Y_{td})	The size of the training dataset (n_{td})	The value of k
$Y_{td} = Y_{glbl}$	$n_{td} = 20$	4
$Y_{td} = Y_{glbl}$	$n_{td} > 20$	$\max\left(z_{20}, \frac{z_{n_{td}}}{n_{td}} \times 20\right) + 1$
$Y_{td} = Y_{lcl,j}$	$n_{td} = 1$	1
$Y_{td} = Y_{lcl,j}$	$1 < n_{td} < 4$	$n_{td} - 1$
$Y_{td} = Y_{lcl,j}$	$n_{td} > 4$	4

Table 4
The mechanism for determining time-dependent room temperature setpoints.

Control mode $CM\,(occ,v_{shrt})$	Predicted occupancy information		Temperature setpoint (T_{sp})
	Time of next presence ($t_{prdct,np}$)	Presence duration of the remaining day ($t_{prdct,drtn}$)	
1			$T_{sp,cmf}$
0	$t_{prdct,np} \in t_{sg,2}$		$T_{sp,dl}$
0	$t_{prdct,np} \in t_{sg,3}$	$t_{prdct,drtn} > t_{drtn,thrd2}$	$T_{sp,dl}$
0	$t_{prdct,np} \in t_{sg,3}$	$t_{drtn,thrd1} \leqslant t_{prdct,drtn} \leqslant t_{drtn,thrd2}$	$T_{sp,ddl}$
0	$t_{prdct,np} \in t_{sg,3}$	$t_{prdct,drtn} < t_{drtn,thrd1}$	$T_{sp,ecn}$
0	$t_{prdct,np} \in t_{sg,4}$	$t_{prdct,drtn} > t_{drtn,thrd2}$	$T_{sp,ddl}$
0	$t_{prdct,np} \in t_{sg,4}$	$t_{prdct,drtn} \leqslant t_{drtn,lmt2}$	$T_{sp,ecn}$
0	$t_{prdct,np} \in t_{sg,5}$		$T_{sp,ecn}$

3. Case study

3.1. Case study building and experimental setup

The case study building located in Singapore is used for commercial purposes, as shown in Fig. 3. The building's construction properties and thermal environment comply with the 2015 Green Mark Platinum Standard for Non-Residential New Buildings per the Singapore Building and Construction Authority [45]. Office spaces in this building are air-conditioned throughout the year during weekdays because of the tropical climate.

The experiment in this research was conducted in 11 rooms on the same floor of the case study building, including typical office scenarios: multi-person offices, single person offices, and meeting rooms. This office space was designed by researchers under the Chair of Architecture and Building Systems at ETH Zürich [46]. As shown in Fig. 4, the total experimental area is around 276 m^2 with 2 multi-person offices, 8 single person offices, and a meeting room. Each room is regarded as a single thermal zone, and its indoor air temperature is controlled by the DCC individually on the basis of occupants' behavior.

For considerations of privacy, labels and data of individual rooms cannot be provided as the floor plan presented in this paper.

All target rooms have the same experimental setup, including sensible cooling systems, environmental sensory infrastructure, and controls. The sensible cooling is delivered by passive chilled beams (PCBs), and room air temperatures are controlled by regulating the chilled water flow rate of PCBs with motorized balancing valves.

For environment and energy perception, each room is equipped with four types of components: (1) motion sensors for analyzing rooms' occupancy, (2) room climate sensors for monitoring temperature, relative humidity, and CO_2 concentration, (3) a human-machine interface (HMI) for occupants to view room temperature and to modify temperature setpoints to their preferences, and (4) energy meter for recording sensible cooling energy usage. Fig. 5 shows photos of this sensory infrastructure, and Table 5 lists the number of them in the entire experimental space. The energy meters were approved in accordance with EN 1434 and measuring instruments directive accuracy class 2 [47].

Fig. 3. Case study building for this research.

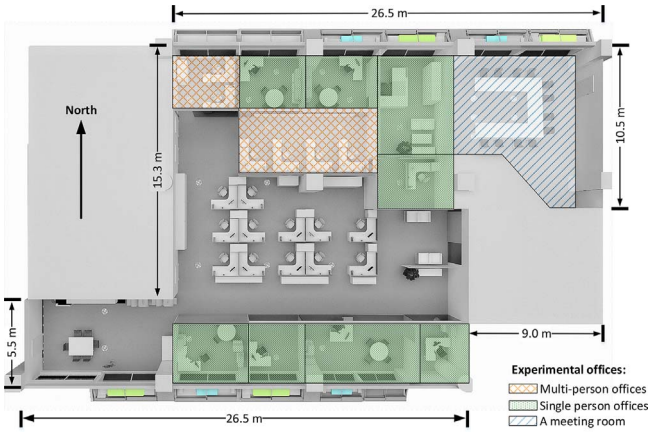

Fig. 4. Floor plan of the case study space.

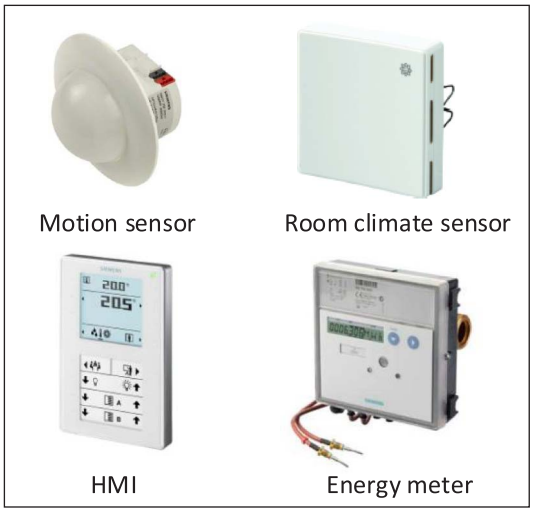

Fig. 5. The components of sensory infrastructure in the case study.

The cooling operation in each single room consists of two layers: (1) local controllers based on proportional-integral-derivative (PID) control, mainly to adjust balancing valves of PCBs to maintain the temperature of an individual room at a defined setpoint level. (2) the DCC strategy, primarily to dynamically specify room temperature setpoints for the first layer by learning from occupants' stochastic behavior in individual rooms.

The proposed DCC algorithm has been developed in a MATLAB client and executed on a workstation computer that has network access to a BMS for collecting sensor data and controlling the local controllers.

Table 5
The total number of sensory infrastructure for the experiment.

Sensory infrastructure	Number of them
Motion sensor	19
Room climate sensor (i.e. for temperature, relative humidity, and CO_2)	34
HMI	11
Energy meter	12

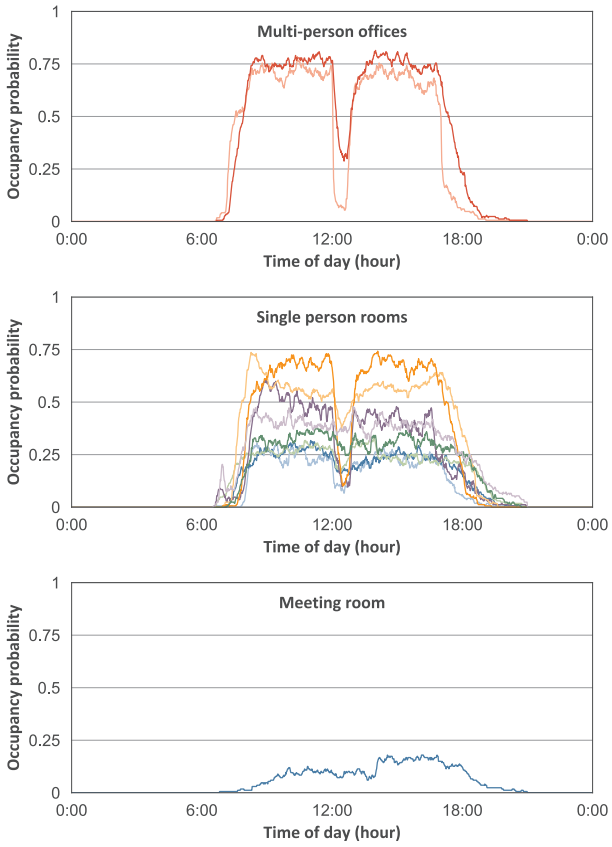

Fig. 6. Weekday occupancy probability distributions (7.5-month data between 2016 and 2017).

3.2. Occupancy-related data

In this study, occupants' movements within each case study room are monitored by motion sensors. After transforming motion sensor measurements of the 11 offices to occupancy data, weekday occupancy probability distributions of the monitored 7.5 months are presented in Fig. 6. The likelihood of occupancy in the rooms differ from each other, and they are mainly classified into three groups according to the office types:

- High occupancy rates in the multi-person offices, and daily occupancy rates are around 0.75.
- Medium occupancy rates in the single person offices, ranging from around 0.25 to 0.75, and likelihoods in six of eight rooms are below 0.5 in most of the daily time.
- Low occupancy rates in the meeting room, the daily occupancy rates are less than 0.25.

As there are low occupancy rates in the meeting room and medium occupancy rates in the single person offices, assignments of setback temperatures during rooms' unoccupied periods would achieve energy savings for the rooms.

As presented in Section 2, the number of occupancy patterns is limited to 4, and the k-means algorithm is applied to cluster occupancy patterns based on two-dimensional data consisting of daily first arrivals and last departures. After extracting the two-dimensional data from the above 7.5-month occupancy dataset, Fig. 7 shows an example of occupancy pattern clusters and related distributions of daily first arrivals and last departures in a case study room. The same learning approach is implemented into the DCC to create the local training datasets.

3.3. Experimental study and examples of control operations

In this study, two experiments were performed in the 11 case study rooms over nine weeks (i.e. 4.5 weeks for each experiment). They are a baseline test and a DCC test described as follows, and the offices used the same comfort temperature setpoint for both tests:

The baseline test is the original control strategy employed by the case study space, using a static operation schedule for the comfort mode. As defined by the building facility department, the case study space is air-conditioned to predefined 'comfort' conditions between 7:00 and 18:00 on weekdays.

The DCC test integrates the proposed methodology into the existing sensible cooling system according to the experimental setup illustrated in Section 3.1. Such control in each office takes over the sensible cooling operation from 8:00 to 18:00 by specifying operation modes together with related room temperature setpoints in real time.

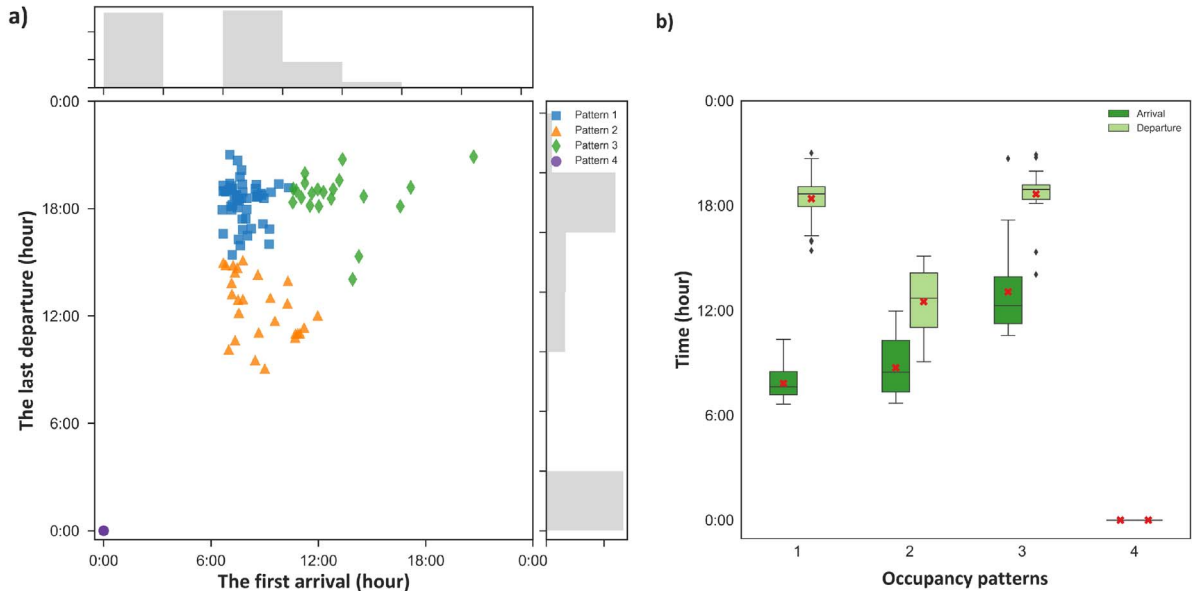

Fig. 7. An example of occupancy patterns in an experimental room (7.5-month data between 2016 and 2017). (a) Four occupancy clusters together with the daily first-arrival histogram (gray bars on the top) and the daily last-departure histogram (gray bars on the right), (b) the first arrival and the last departure distributions (box plot) and mean values (red cross) for four occupancy clusters. (For interpretation of the references to colour in this figure legend, the reader is referred to the web version of this article.)

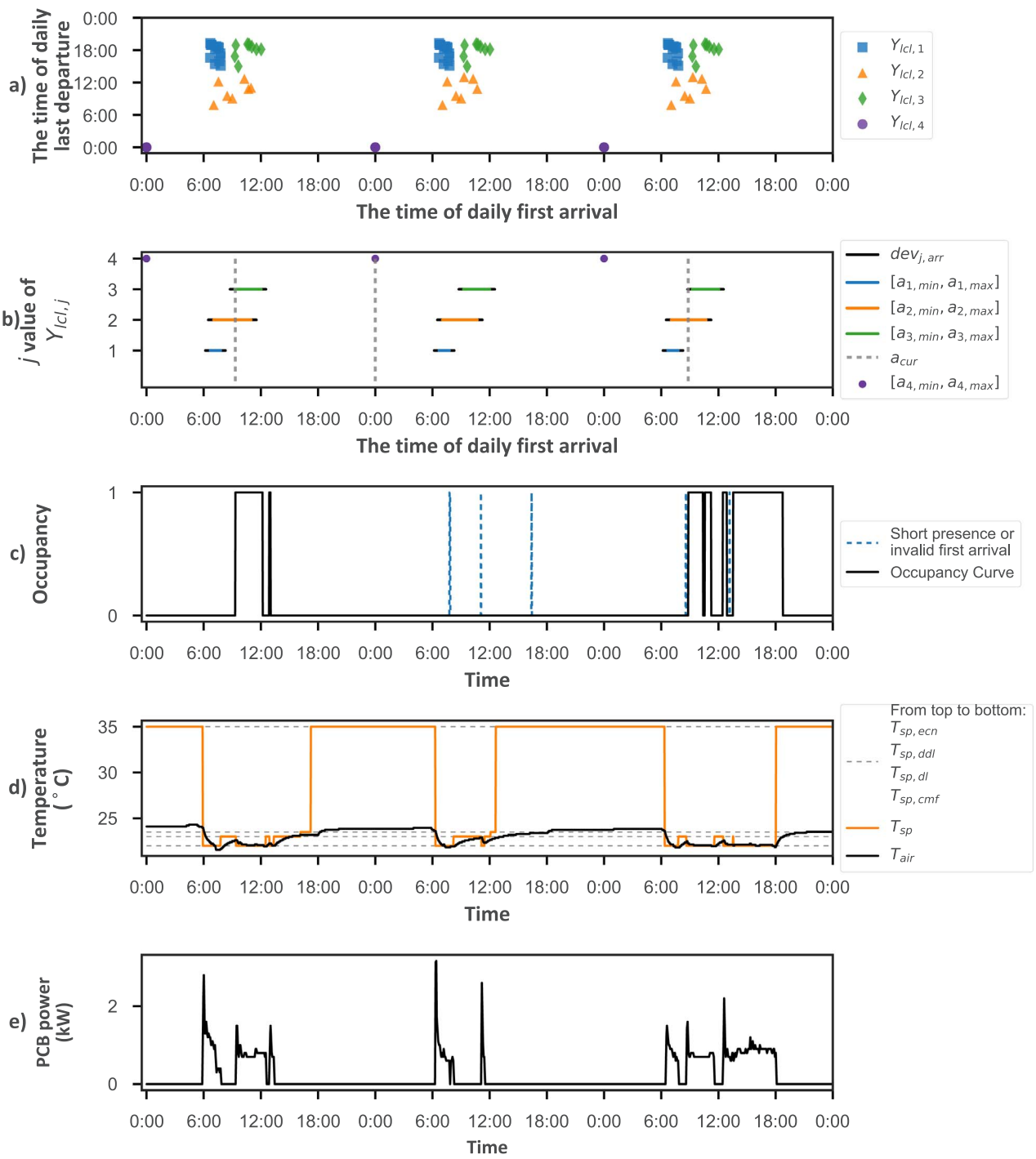

Fig. 8. An example of the three-day DCC operations in a case study office. (a) Local training datasets $Y_{lcl,j}$, (b) time ranges of daily first arrivals of $Y_{lcl,j}$ (i.e. $[a_{j,min}, a_{j,max}]$) and their deviations (i.e. $dev_{j,arr}$) as well as the valid first arrival time in experimental days (i.e. a_{cur}), (c) occupancy curve in experimental days, d) temperature setpoints generated by the DCC (i.e. T_{sp}), room air temperature T_{air}, and four temperature levels for comfort and setback modes (i.e. $T_{sp,cmf}$, $T_{sp,dl}$, $T_{sp,ddl}$, and $T_{sp,ecn}$), (e) PCB sensible cooling power.

Setpoints of the comfort mode (i.e. assumed 'comfort' conditions) are defined by the building facility: two rooms are set to 22 °C, and the other nine rooms are set to 22.5 °C.

For the DCC operation, two successful examples from two rooms are depicted in Figs. 8 and 9, respectively. Each figure presents three-day operations with five subgraphs. In the early phase of DCC operation per day, it selects the global training dataset from historical occupancy data, and then starts the first learning process to cluster occupancy patterns with k-means for local training datasets, as shown in (a). Meanwhile, the time ranges or points (i.e. first arrivals only occur at a time point) of daily first arrivals of the local training datasets are calculated, as presented in (b). After the DCC starts inferring real-time room temperature setpoints, it closely monitors occupancy status in each case study room as shown in (c), and it recognizes the valid daily first arrival in the current day for defining the final training data for the second learning process. As shown in (b), when the daily first arrival in the current day falls into one or several arrival time ranges or points together with their deviations of the local training datasets, these designated local training datasets are regarded as the final training data. The global training dataset is used as the training data when there is no valid daily first arrival, or the maximum vacancy duration of the current occupancy vector is larger than thresholds of adopted local

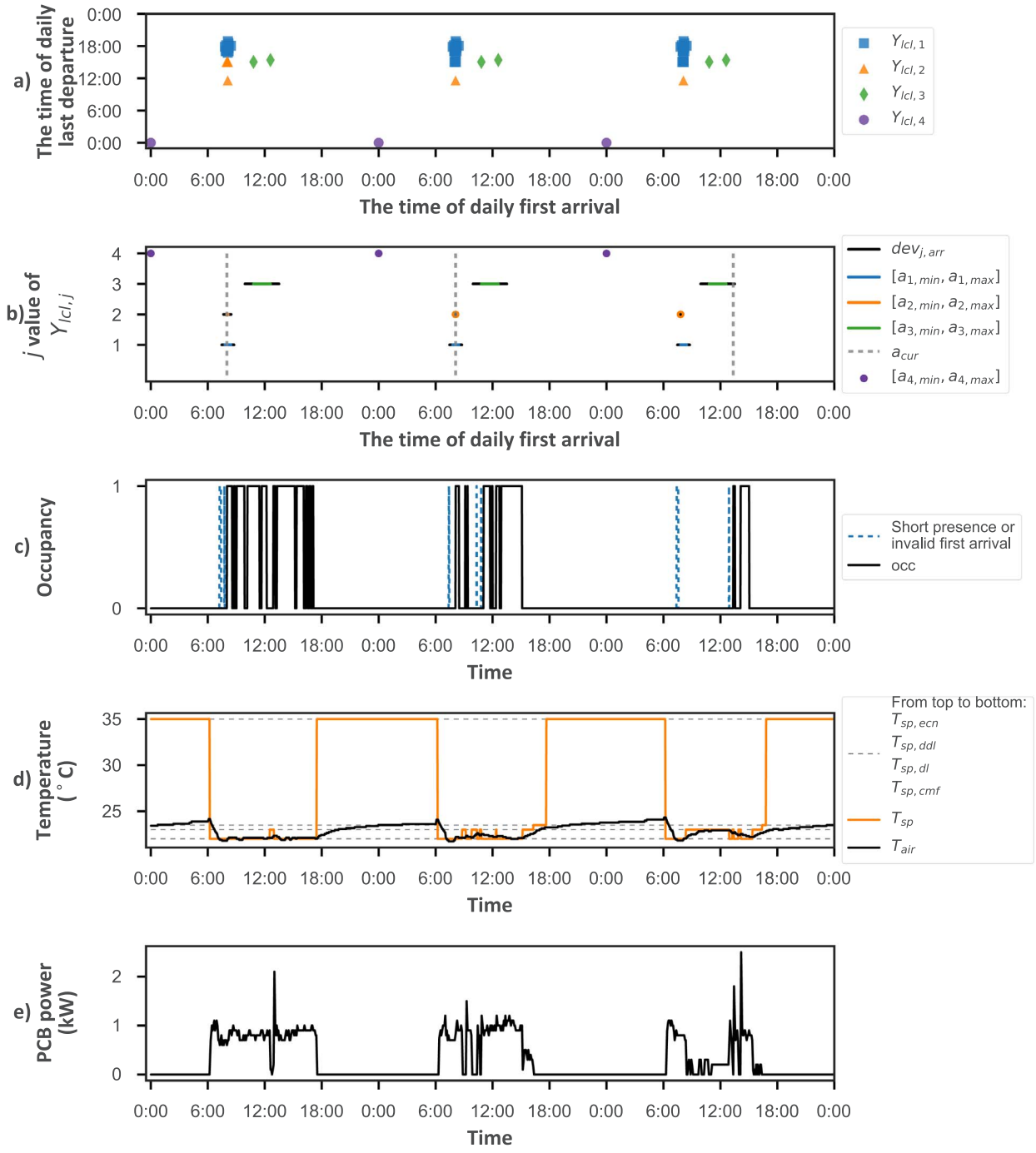

Fig. 9. An example of the three-day DCC operations in another case study office. (a) Local training datasets $Y_{lcl,j}$, (b) the time ranges of daily first arrivals of $Y_{lcl,j}$ (i.e. $[a_{j,min}, a_{j,max}]$) and their deviations (i.e. $dev_{j,arr}$) as well as the first arrival time in experimental days (i.e. a_{cur}), (c) occupancy curve in experimental days, (d) temperature setpoints generated by the DCC (i.e. T_{sp}), room air temperature T_{air}, and four temperature levels for comfort and setback modes (i.e. $T_{sp,cmf}$, $T_{sp,dl}$, $T_{sp,ddl}$, and $T_{sp,ecn}$), (e) PCB sensible cooling power.

occupancy datasets. Subgraph (d) shows real-time temperature setpoints generated by the DCC together with actual room temperatures. Curves of sensible cooling power are shown in subgraphs (e).

4. Experimental results

This section presents experimental results of the proposed methodology applied to the case study offices from five aspects. Evaluation of control accuracy is presented at the beginning. Analysis of the comfort and setback operations as wells as energy use and savings are illustrated, respectively. Cooling energy consumed by switching control from the setback mode to comfort mode for short presence is also analyzed. Controlled room temperatures are evaluated and presented lastly.

4.1. Evaluation of control accuracy

As occupants' behavior is highly stochastic in offices, the information learned from the learning processes are used indirectly to deduce three setback temperature setpoints based on the rules specified in Table 4: forecasted presence falls into which time range, and occupancy duration is less or greater than the constraints. Thus, the accuracy evaluation is based on the entire DCC strategy. To achieve this purpose, two sets of evaluations with 1-min sampling time are carried out

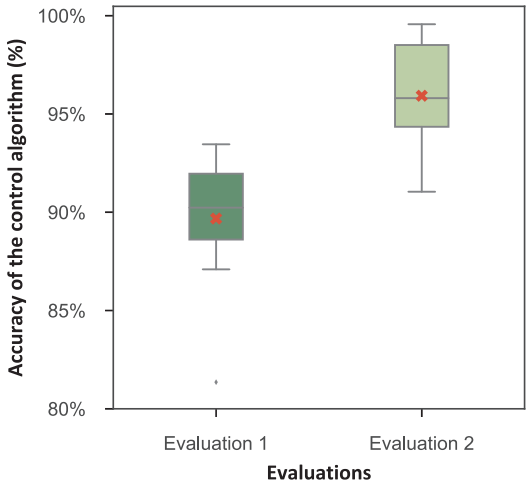

Fig. 10. Distributions (box plot) and mean values (cross) of the DCC control accuracy in the case study offices.

according to specified room temperature setpoints and PCB power data. The first evaluation (i.e. evaluation 1) calculates the control accuracy according to Table 4 from the point of view of the real-time temperature setpoints. The accuracy calculation of the second evaluation (i.e. evaluation 2) is based on both the real-time temperature setpoints and PCB power. For evaluation 2, if the daily last departure (i.e. t_{dprtr}) occurs after $t_{dcc,stp}$, the accuracy calculation is the same as in evaluation 1. If t_{dprtr} occurs between $t_{dcc,strt}$ and $t_{dcc,stp}$, evaluation 2 calculates errors in two time segments respectively: [$t_{dcc,strt}$, t_{dprtr}] and (t_{dprtr}, $t_{dcc,stp}$]. First, control errors during [$t_{dcc,strt}$, t_{dprtr}] are determined by the real-time temperature setpoint, like in evaluation 1. Second, the control errors during (t_{dprtr}, $t_{dcc,stp}$] are calculated by the real-time PCB power: error is set to 0 when no PCB power is consumed with the setback temperatures, otherwise error is set to 1. The overall accuracy of the evaluation 2 is cacluated from the errors of these two time segments.

Fig. 10 illustrates distributions (box plot) and means (cross) of the control accuracy in the case study offices based on evaluation 1 and evaluation 2. The mean control accuracy of evaluation 1 is close to 90%, and the mean control accuracy of evaluation 2 is over 95%. As shown in Figs. 8 and 9, the DCC sets temperature setpoints from $T_{sp,dl}$ to $T_{sp,ddl}$ and when t_{dprtr} occurs earlier. For this scenario, evaluation 1 sets the error to 0 only when temperature setpoints are assigned by , and evaluation 2 sets the error to 0 when no PCB power is consumed. From actual energy perspective, the DCC effectively shuts down cooling systems after the t_{dprtr} with increasing setback setpoints step by step as the probability of occupants presents in an office goes down.

4.2. Ratios of the comfort mode and the setback mode

Before stating results of the energy savings achieved by the DCC operation, we analyze operation ratios of the comfort and setback modes in the 11 case study offices over the entire DCC test period. Two control modes (i.e. comfort and setback) with four temperature setpoints were employed to control room temperature for the purpose of saving energy and maintaining comfortable room temperature for occupants. As shown in Figs. 8 and 9, the sensible cooling energy savings are contributed by the setback mode. The average operation ratios of the four setpoints in the 11 case study offices are presented in ways of distributions (box plot) and means (cross), as shown in Fig. 11. It can be observed that four temperature setpoints of the setback mode were deployed in all the experimental offices by the DCC.

4.3. Energy use and savings

The energy consumption of the sensible cooling in the case study

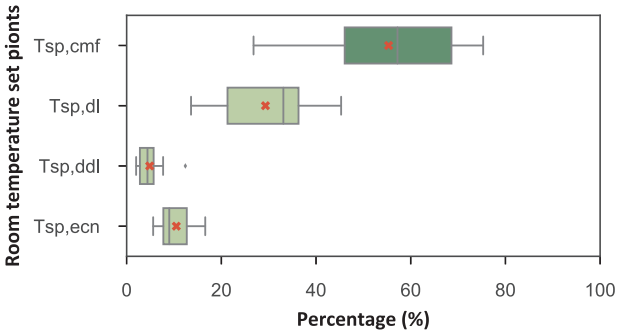

Fig. 11. Distributions (box plot) and mean values (cross) of average operation ratios of $T_{sp,cmf}$, $T_{sp,dl}$, $T_{sp,ddl}$, and $T_{sp,ecn}$ in the 11 case study offices during the DCC experiment.

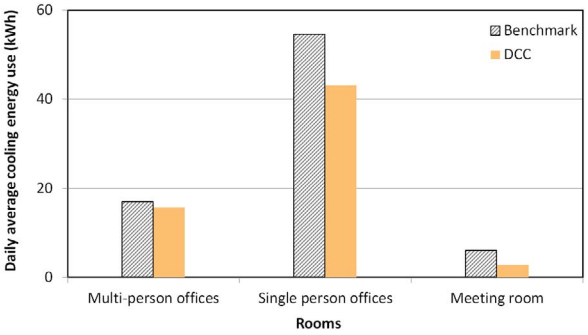

Fig. 12. Normalized daily average sensible cooling energy use in three types of offices during the experiments.

rooms is calculated from energy meters installed in PCBs pipe networks of the case study space. For evaluating energy savings with deploying the DCC into the cooling systems, the energy use in the baseline test is employed to calculate energy benchmarks according to a normalization method presented in [6]. For minimizing energy impact caused by energy patterns associated with the day of the week, the baseline and DCC tests were deployed on weekdays with the same number of days of the week.

For three types of rooms in the case study space, Fig. 12 presents daily average sensible cooling consumption of the benchmark and the DCC, and Table 6 shows energy savings of each type of offices and the entire space achieved by the DCC.

The experimental results showed that the DCC operation successfully reduced the sensible energy use by making cooling service automatically adapt to actual energy demands in real time. They also indicated that the energy savings potential was inversely correlated with occupancy rates within three types of rooms.

The energy savings in the multi-person offices were only 7% because of the high occupancy rates presented in Section 3.2. For the single person offices with medium occupancy rates, a 21% reduction was achieved. As daily occupancy rate in the meeting room is even below 25%, the energy saving touched a high point: 52%. Across the 11 offices, the DCC saved 21% of the sensible cooling energy with reducing unnecessary energy requirements during vacancy periods.

Table 6
Sensible cooling energy savings in three types of offices and the entire space during the DCC test.

	Multi-person offices	Single person offices	Meeting room	The entire space
Energy savings (%)	7%	21%	52%	21%

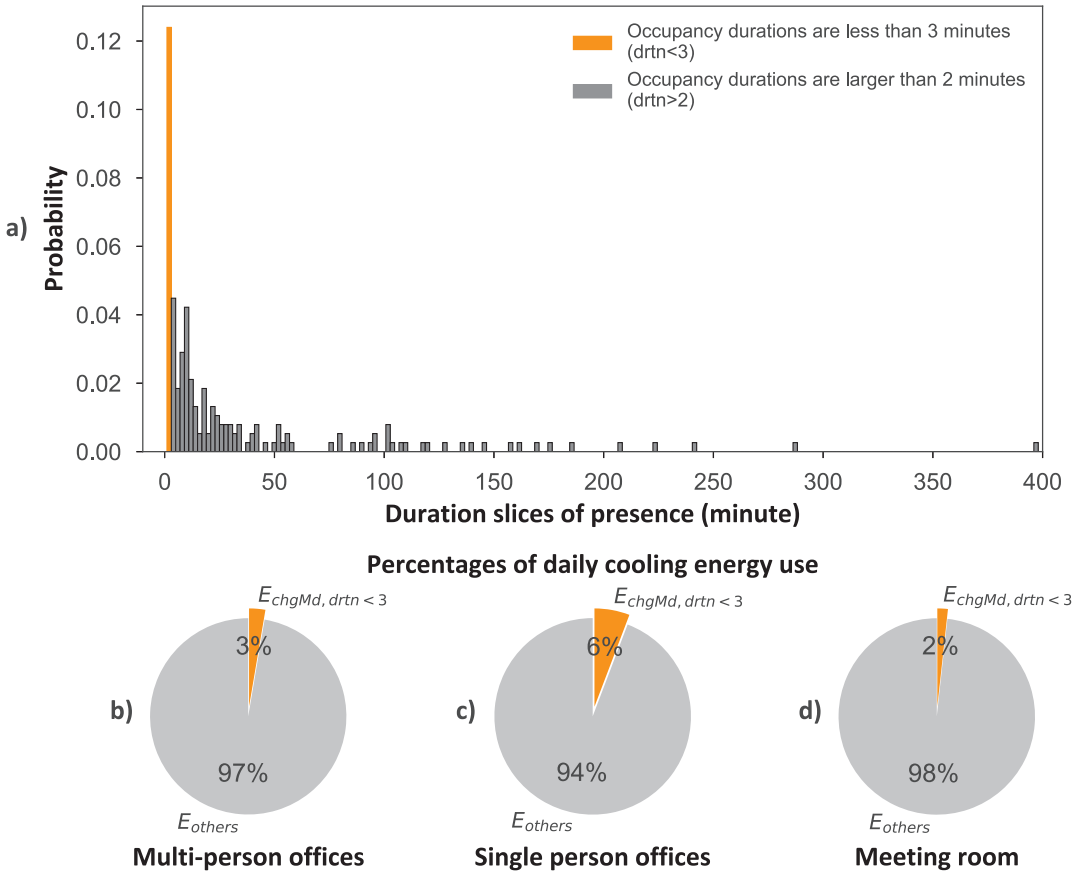

Fig. 13. Analysis of short stays and energy consumed by switching control from $T_{sp,dl}$ and $T_{sp,ddl}$ to the comfort mode for short stays during the DCC test. (a) Probabilities of occupancy duration slices in the entire experimental rooms, (b) to (d) ratios of daily cooling energy consumption in the multi-person offices, the single person offices, and the meeting room.

4.4. Cooling energy consumed by switching control modes for short presence

In this study, a function is embedded into the DCC structure to recognize short presence – occupancy duration is less than 3 mins ($drtn < 3$) – to avoid cooling down the rooms unnecessarily. However, it is only enabled when the setback mode employs as the setpoint, that is, the DCC keeps as the setpoint when presence is a short stay. In the other setback conditions (i.e. $T_{sp,dl}$ and $T_{sp,ddl}$), this function is disabled and the DCC reverts to the comfort mode once an occupant showed up in an office. It is primarily to make the cooling operation respond to the presence of an occupant quickly.

Rooms are usually occupied in segments with various lengths of time in the daily time frame. As shown in Fig. 13(a), however, short presence in the case study offices (orange bar) accounted for a large ratio of the overall occupancy slices. Cooling energy consumed by changing temperature setpoints from $T_{sp,dl}$ and $T_{sp,ddl}$ to the comfort mode for such short stays ($E_{chgMd,drtn<3}$) cannot be neglected. As shown in Fig. 13(b)–(d), $E_{chgMd,drtn<3}$ accounted for 3%, 6%, and 2% of daily cooling energy consumption in the multi-person offices, the single person offices, and the meeting room, respectively. Across the entire case study space, $E_{chgMd,drtn<3}$ took 5% of daily cooling energy. If the DCC keeps room temperature setpoints at $T_{sp,dl}$ or $T_{sp,ddl}$ when short stays occur in the setback mode, more energy savings can be achieved under the condition that occupants are assumed not to be concerned with room temperature during such momentary periods.

4.5. Controlled room temperature

As well as saving cooling energy of the offices, ensuring that the occupants in the experimental spaces are thermally comfortable is also one of the main objectives of this study. Each case study room is equipped with climate sensors to monitor indoor air temperatures in real time, and an HMI to let the occupants check their room temperatures and override setpoint temperatures according to their preferences.

To analyze and compare room temperatures controlled by the baseline (i.e. originally scheduled cooling operation) and DCC tests during occupied periods, we extracted the indoor air temperature of each occupied minute from the 11 rooms. Then, for each occupied minute, a temperature difference between the actual temperature of a room and corresponding $T_{sp,cmf}$ is computed. Fig. 14 presents distributions (box plot) and means (cross) of these temperature deviations for the baseline and DCC tests.

The results show that means of temperature deviations in the baseline and DCC tests are very close: differences between their deviations are all less than 0.1 °C in the three types of case study rooms.

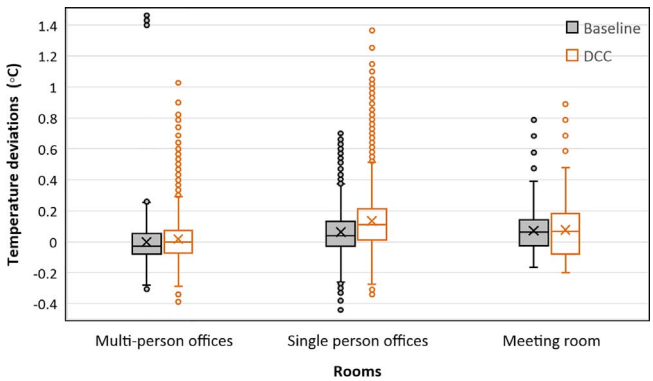

Fig. 14. Distributions (box plot) and means (cross) of temperature deviations during occupied periods with a 1-min resolution between 8:00 to 18:00.

This indicates that the DCC operation showed good control performance for maintaining room temperatures to $T_{sp,cmf}$ during occupied periods, similar to that controlled by the original scheduled cooling strategy. For the distributions of the temperature deviations, the majority of the deviations are controlled within 0.5 °C by both baseline and DCC operations, and only outliers are beyond that range.

To investigate whether the occupants intend to override the room temperatures controlled by the DCC operation, we collected setpoint shifts modified by the occupants (i.e. occupants' feedback on controlled temperature) with HMIs. Data shows that the time-dependent temperatures controlled by the DCC were not adjusted by the occupants in the 11 rooms throughout the whole DCC experiment.

5. Discussion

This section discusses advantages and limitations of this study. The proposed DCC methodology has the following attractive traits.

In present-day demand-driven building control, occupancy signals transformed from motion sensors are based on basic Boolean attribute in the timeline. In this study, we deconstructed binary-based occupancy vectors into three dimensions as shown in Fig. 15: (1) time-based features, (2) quantitative features, and (3) deviation features. All three dimensions were embedded into two proposed learning processes of the DCC. Hence, the DCC in this study not only integrated occupants' original behavior (i.e. the first two types of features), but also considered deviations of their daily behavior (i.e. the third type of feature) to enhance the control reliability in light of the uncertain stochastic behavior of occupants.

Second, we suggested two types of training datasets for the occupancy learning process: the global and local training datasets. The local training datasets are used to reduce control errors caused when k-most-closest neighbors that are picked from the global training dataset are not similar to the occupancy pattern in the current day. Meanwhile, the global training dataset effectively makes the DCC respond to changes of the occupancy pattern in the current day, such as when the current occupancy pattern deviates from the local training datasets as time goes on during the daily control.

Third, the DCC not only learns occupants' next presence, but also learns the presence duration of the remaining day. Considering the occupants' behavior is highly stochastic in offices [6], these two pieces of occupancy information are only employed indirectly to deduce setback temperature setpoints according to our summarized rules in Table 4. Additionally, three setback temperature setpoints enabled the DCC to increase room temperature step by step as the probability of a room not being occupied decreases for saving energy without compromising room temperatures during occupied periods.

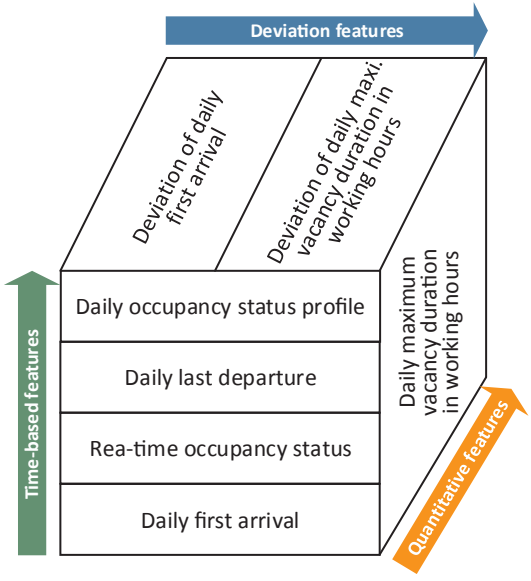

Fig. 15. The occupancy-related features in the three dimensions for the DCC.

Finally, it is important to highlight that the proposed DCC is an active learning methodology, making the cooling system automatically adapt to different office conditions with fewer human interventions during the implementation phase. Two machine learning techniques, k-means and KNN, are embedded in the DCC to give it learning capabilities. Hyperparameters of these learning algorithms are specified in this study: the number of clusters (k_{pttrn}) and the size of training dataset (Y_{glbl}) for k-mean, and the number of nearest neighbors (k) for KNN. In the meantime, the key datasets (i.e. the global, local, and the final training datasets), occupancy-related variables, and room temperature setpoints are spontaneously learned and updated either every day or every few minutes by the learning algorithms and the rules summarized in this study. To generalize the DCC for diverse application requirements and to port this methodology to other systems easily, we pack three sets of variables with six parameters into an initialization function, and only these parameters are required to be configured by end users: definitions of the DCC operation period, threshold values of first arrivals and last departures, and threshold values of presence durations. The first type is specified by end users according to their energy policies, the last two types are mainly linked to their energy-conscious perspectives as we presented in Section 2.5.

In contrast to the above advantages, our study also has some limitations as follows.

The motion sensors used in the case study building apply a change of value method to sample movement signals. A static period (i.e. 10 mins) was applied to interpret motion data in terms of occupancy due to high cumulative probabilities of short inactivity slices (i.e. less than 100 ss) created by such sampling method. However, for motion sensors with other sampling methods (e.g. integrating a delay time setting to maintain a captured status for a minimum duration after detecting motions), adaptive periods that transform motion data to occupancy information can offer an opportunity to further reduce energy consumption [35]. To make the DCC generic, both static and adaptive periods could be integrated into the control strategy to reflect motion sensors with different sampling methods.

The case study building is used for commercial purposes, so the tests in this paper were conducted over 9 weeks in the 11 offices. The experimental time and the number of the case study offices are not significant in contrast to product-ready control systems. Both may limit the generalizability of the results illustrated in this paper. Though this study faces such limitations, the real-world offices evaluated by this work captured high variations in occupants' behavior across three main office scenarios: single person office, multi-person office, and meeting room. This was enough to explore the inverse correlation between energy savings and occupancy rates as well as how building energy use can be reduced by a DCC operation without compromising room temperatures during occupied periods in practice.

6. Conclusions

The methodology illustrated in this paper has been successfully conducted under real-world conditions in 11 rooms of a commercial building. The experimental results show that a 7–52% energy saving was obtained by the adaptive cooling system, depending on occupancy rates, with average savings in the order of 21% across the entire space, as compared to using the conventional control system. The reviewed occupancy demand-driven HVAC systems with machine learning techniques presented 8–28% energy reductions, which is a similar range to the achieved energy savings of this study. It was further found, at least in this study, that the achieved energy savings are inversely correlated to the occupancy rates of individual rooms.

Energy could have been further saved by forcing the setback

temperature setpoints to be maintained when short presences are detected in setback mode. Short presence frequently occurs in the offices as analyzed in Section 4.4. In this study, a short-presence-detection function is employed to recognize if a current presence is a brief stay or not. This function needs 12 mins to finish the recognition, which is rather long. It was therefore only applied to avoid cooling down the rooms for short stays that occur when is assigned to the setback mode. However, from the assessment shown in Section 4.4, about 2% to 6% further energy saving could be achieved further by maintaining the setback temperature setpoints instead of reverting to the comfort mode when short presence occurs in the setback modes with $T_{sp,dl}$ and $T_{sp,ddl}$. An advanced sensor network that could quickly identify whether a presence is short or not would be the future work to realize these additional energy savings.

During occupied periods, the means of temperature deviations in the DCC test phase is less than 0.1 °C against conditions measured during the baseline test phase. We did not observe that the occupants of the 11 offices overrode the DCC-controlled room temperature with HMIs either.

According to the above experimental results, it is safe to assume that the proposed control methodology not only reduces cooling energy use, but also does not compromise room temperatures during occupied periods.

In this paper, a machine-learning-based cooling control strategy for office buildings was proposed. The proposed control strategy is not limited to space cooling control, but could also be extended to heating and ventilation control using the same methodology to infer humidity and CO_2 concentration setpoints. Complicated algorithms may be difficult to embed into local controllers due to limits of memory and computing [48]. For controlling HVAC systems of a much larger number of rooms, it is possible to integrate the proposed DCC in existing computer-based BMS as an application function.

Acknowledgements

The authors would like to thank Siemens Building Technologies and United World College South East Asia for their support of this research.

References

[1] Pérez-Lombard L, Ortiz J, Coronel JF, Maestre IR. A review of HVAC systems requirements in building energy regulations. Energy Build 2011;43:255–68. http://dx.doi.org/10.1016/j.enbuild.2010.10.025.
[2] Yang L, Yan H, Lam JC. Thermal comfort and building energy consumption implications – a review. Appl Energy 2014;115:164–73. http://dx.doi.org/10.1016/j.apenergy.2013.10.062.
[3] Chua KJ, Chou SK, Yang WM, Yan J. Achieving better energy-efficient air conditioning – a review of technologies and strategies. Appl Energy 2013;104:87–104. http://dx.doi.org/10.1016/j.apenergy.2012.10.037.
[4] Hong T, Yan D, D'Oca S, Chen C. Ten questions concerning occupant behavior in buildings: the big picture. Build Environ 2017;114:518–30. http://dx.doi.org/10.1016/j.buildenv.2016.12.006.
[5] Mahdavi A, Mohammadi A, Kabir E, Lambeva L. Occupants' operation of lighting and shading systems in office buildings. J Build Perform Simul 2008;1:57–65. http://dx.doi.org/10.1080/19401490801906502.
[6] Peng Y, Rysanek A, Nagy Z, Schlüter A. Occupancy learning-based demand-driven cooling control for office spaces. Build Environ 2017;122:145–60. http://dx.doi.org/10.1016/j.buildenv.2017.06.010.
[7] Masoso OT, Grobler LJ. The dark side of occupants' behaviour on building energy use. Energy Build 2010;42:173–7. http://dx.doi.org/10.1016/j.enbuild.2009.08.009.
[8] Nguyen TA, Aiello M. Energy intelligent buildings based on user activity: a survey. Energy Build 2013;56:244–57. http://dx.doi.org/10.1016/j.enbuild.2012.09.005.
[9] IEA. World Energy Outlook 2015. Paris: Organisation for Economic Co-operation and Development; 2015.
[10] IEA. World Energy Outlook 2016. Paris: Organisation for Economic Co-operation and Development; 2016.
[11] Labeodan T, Zeiler W, Boxem G, Zhao Y. Occupancy measurement in commercial office buildings for demand-driven control applications—a survey and detection system evaluation. Energy Build 2015;93:303–14. http://dx.doi.org/10.1016/j.enbuild.2015.02.028.
[12] Peng Y, Rysanek A, Nagy Z, Schlüter A. Case study review: prediction techniques in intelligent HVAC control systems. In: 9th Int conf indoor air qual vent energy conserv build, Songdo, Incheon. Republic of Korea: n.d.
[13] Michael C. Mozer, Vidmar L, Dodier RH. The neurothermostat: Predictive optimal control of residential heating systems. Adv Neural Inf Process Syst 1997:953–9.
[14] Scott J, Bernheim Brush AJ, Krumm J, Meyers B, Hazas M, Hodges S, et al. PreHeat: Controlling home heating using occupancy prediction. In: Proc 13th int conf ubiquitous comput, New York, NY, USA: ACM; 2011. p. 281–290. 10.1145/2030112.2030151.
[15] Kadouche R, Chikhaoui B, Abdulrazak B. User behavior study for smart houses occupant prediction. Ann Telecommun – Ann Télécommun 2010;65:539–43. http://dx.doi.org/10.1007/s12243-010-0166-2.
[16] Sangogboye FC, Imamovic K, Kjærgaard MB. Improving occupancy presence prediction via multi-label classification. In: 2016 IEEE int conf pervasive comput commun Workshop PerCom Workshop; 2016. p. 1–6. 10.1109/PERCOMW.2016.7457147.
[17] Ortega JLG, Han L, Whittacker N, Bowring N. A machine-learning based approach to model user occupancy and activity patterns for energy saving in buildings. Sci Inf Conf SAI 2015:474–82. http://dx.doi.org/10.1109/SAI.2015.7237185.
[18] Chaney J, Hugh Owens E, Peacock AD. An evidence based approach to determining residential occupancy and its role in demand response management. Energy Build 2016;125:254–66. http://dx.doi.org/10.1016/j.enbuild.2016.04.060.
[19] Bing D. Integrated Building Heating, Cooling and Ventilation Control PhD Thesis Carnegie Mellon University; 2010
[20] Bing D, Poh Lam Khee. A real-time model predictive control for building heating and cooling systems based on the occupancy behavior pattern detection and local weather forecasting. Build Simul 2014;7:89–106.
[21] Wang W, Chen J, Huang G, Lu Y. Energy efficient HVAC control for an IPS-enabled large space in commercial buildings through dynamic spatial occupancy distribution. Appl Energy 2017. http://dx.doi.org/10.1016/j.apenergy.2017.06.060.
[22] Ryu SH, Moon HJ. Development of an occupancy prediction model using indoor environmental data based on machine learning techniques. Build Environ 2016;107:1–9. http://dx.doi.org/10.1016/j.buildenv.2016.06.039.
[23] Yang Z, Li N, Becerik-Gerber B, Orosz M. A multi-sensor based occupancy estimation model for supporting demand driven HVAC operations. In: Proc 2012 symp simul archit urban des, San Diego, CA, USA: Society for Computer Simulation International; 2012. p. 2:1–2:8.
[24] Mamidi S, Chang Y-H, Maheswaran R. Improving building energy efficiency with a network of sensing, learning and prediction agents. In: Proc 11th int conf auton agents multiagent syst – vol. 1, Richland, SC: International Foundation for Autonomous Agents and Multiagent Systems; 2012. p. 45–52.
[25] Ekwevugbe T, Brown N, Pakka V, Fan D. Real-time building occupancy sensing using neural-network based sensor network. In: 2013 7th IEEE int conf digit ecosyst technol DEST; 2013. p. 114–9. 10.1109/DEST.2013.6611339.
[26] Chen Z, Soh YC. Comparing occupancy models and data mining approaches for regular occupancy prediction in commercial buildings. J Build Perform Simul 2016:1–9. http://dx.doi.org/10.1080/19401493.2016.1199735.
[27] Liang X, Hong T, Shen GQ. Occupancy data analytics and prediction: a case study. Build Environ 2016;102:179–92. http://dx.doi.org/10.1016/j.buildenv.2016.03.027.
[28] Capozzoli A, Piscitelli MS, Gorrino A, Ballarini I, Corrado V. Data analytics for occupancy pattern learning to reduce the energy consumption of HVAC systems in office buildings. Sustain Cities Soc 2017;35:191–208. http://dx.doi.org/10.1016/j.scs.2017.07.016.
[29] Lu J, Sookoor T, Srinivasan V, Gao G, Holben B, Stankovic J, et al. The smart thermostat: using occupancy sensors to save energy in homes. In: Proc 8th ACM conf embed networked sens syst, New York, NY, USA: ACM; 2010. p. 211–24. 10.1145/1869983.1870005.
[30] Kleiminger W, Mattern F, Santini S. Predicting household occupancy for smart heating control: a comparative performance analysis of state-of-the-art approaches. Energy Build 2014;85:493–505. http://dx.doi.org/10.1016/j.enbuild.2014.09.046.
[31] D'Oca S, Hong T. Occupancy schedules learning process through a data mining framework. Energy Build 2015;88:395–408. http://dx.doi.org/10.1016/j.enbuild.2014.11.065.
[32] A First Encounter with Machine Learning. Goodreads, n.d. < http://www.goodreads.com/work/best_book/25591268-a-first-encounter-with-machine-learning > [accessed December 22, 2015].
[33] Hal Daumé III. Unsupervised Learning. Httpcimlinfodlv09ciml-V09-Ch13pdf; 2014.
[34] Krumm J, Brush AJB. Learning time-based presence probabilities. In: Lyons K, Hightower J, Huang EM, editors. Pervasive comput. Berlin Heidelberg: Springer; 2011. p. 79–96.
[35] Nagy Z, Yong FY, Frei M, Schlueter A. Occupant centered lighting control for comfort and energy efficient building operation. Energy Build 2015;94:100–8. http://dx.doi.org/10.1016/j.enbuild.2015.02.053.
[36] Dong B. Sensor-based occupancy behavioral pattern recognition for energy and comfort management in InTELligent Buildings, n.d.
[37] Burak Gunay H, O'Brien W, Beausoleil-Morrison I. Development of an occupancy learning algorithm for terminal heating and cooling units. Build Environ, n.d. 10.1016/j.buildenv.2015.06.009.
[38] Chandrashekar G, Sahin F. A survey on feature selection methods. Comput Electr Eng 2014;40:16–28. http://dx.doi.org/10.1016/j.compeleceng.2013.11.024.
[39] Harrington P. Machine Learning in Action. 1st ed. Shelter Island, N.Y: Manning Publications; 2012.
[40] Alex S, S.V.N. V. Introduction to Machine Learning. Cambridge University Press; 2008.
[41] Wu X, Kumar V, Quinlan JR, Ghosh J, Yang Q, Motoda H, et al. Top 10 algorithms in data mining. Knowl Inf Syst 2008;14:1–37. http://dx.doi.org/10.1007/s10115-007-0114-2.

[42] A Course in Machine Learning, n.d. < http://ciml.info/ > [accessed December 23, 2016].
[43] Barber D. Bayesian reasoning and machine learning. New York, NY, USA: Cambridge University Press; 2012.
[44] MacKay DJC. Information theory, inference and learning algorithms. 1st ed. Cambridge, UK; New York: Cambridge University Press; 2003.
[45] Singapore Government, BCA Green Mark for New Non-Residential Buildings Version NRB/4.1, n.d.
[46] Schlueter A, Rysanek A, Miller C, Pantelic J, Meggers F, Mast M, et al. 3for2: Realizing Spatial, Material, and Energy Savings through Integrated Design. CTBUH J; 2016.
[47] EN Standard, EN-1434:Thermal energy (Btu meter or heat meter), n.d.
[48] ASHRAE. 2011 ASHRAE Handbook - HVAC Applications - IP. Atlanta, Ga.: Refrigerating and Air-Conditioning Engineers, American Society of Heating; 2011.